Structural Optimization 16, 280–288 © Springer-Verlag 1998

A systematic topology optimization approach for optimal stiffener design

J. Luo and H.C. Gea
Department of Mechanical and Aerospace Engineering, Rutgers, The State University of New Jersey, Piscataway, NJ 08855-0909, USA

Abstract A systematic topology optimization based approach is proposed to design the optimal stiffener of three-dimensional shell/plate structures for static and eigenvalue problems. Optimal stiffener design involves the determination of the best location and orientation. In this paper, the stiffener location problem is solved by a microstructure-based design domain method and the orientation problem is modelled as an optimization orientation problem of equivalent orthotropic materials, which is solved by a newly developed energy-based method. Examples are presented to demonstrate the application of the proposed approach.

1 Introduction

Shell/plate structures have been used intensively in the automobile and aerospace industries because they are lightweight and easy to form into the desired shape. However, they often exhibit poor stiffness as well as NVH (noise, vibration and harshness) performance due to their flexibility. One common and cost-effective approach to improving the stiffness and NVH performance of shell/plate structures is the addition of stiffeners, which supplements the rigidity of base structures by increasing their moment of inertia of cross-sections. The design of stiffeners involves the determination of location and orientation of the added stiffeners. To obtain the maximum advantage from the added stiffeners, both location and orientation of stiffeners must be placed optimally. In the past, the stiffener location problem has been investigated intensively using various topology optimization approaches (Diaz and Kikuchi 1992; Ma *et al.* 1993; Yang and Chahande 1995). However, the optimal stiffener orientation still remains uncertain. In this paper, a systematic topology optimization approach is proposed to obtain the optimal location and orientation of stiffener design for 3D shell/plate structures.

The proposed approach involves a two-phase procedure that utilizes a mathematical programming method for solving the optimal location problem and then uses an analytically-based optimality criteria method for the optimal orientation. In the first phase, the optimal location of stiffeners is to be identified. A microstructure-based design domain method (Gea 1996) is employed to formulate this problem and that is solved iteratively by a sequential convex approximation method called generalized convex approximation (Chickermane and Gea 1996). In the second phase, the optimal stiffener orientation problem is considered. A bending equivalent orthotropic material model is proposed to transform a stiffener orientation problem into an optimal orientation problem of equivalent orthotropic materials, which is solved by an analytically-based optimality criteria method (Luo and Gea 1997).

The remainder of the paper is organized as follows. Section 2 deals with the stiffener location problem, where the microstructure-based design domain method is briefly discussed and the sensitivity analysis and problem formulation are derived. The stiffener orientation problem is considered in Section 3, in which an equivalent orthotropic model is introduced first and the optimality conditions of the stiffener orientation are then derived. An energy-based method is also briefly discussed in Section 3. Section 4 presents the numerical results of the proposed method. Some concluding remarks are made in the last section.

2 Phase I: optimal stiffener location

In the first phase, the stiffener location problem is treated as an optimal distribution problem of given stiffener materials on the base structure to achieve the stiffest structure under static loading or dynamic excitation. In the past decade, various methods have been developed to deal with the optimal material distribution problems. One of the earlier approaches is the homogenization method which is based on the homogenization theory to obtain the homogenized material properties (Bendsøe and Kikuchi 1988). Another popular approach is the density function approach (Bendsøe 1989; Rozvany and Zhou 1990; Mlejnek and Schirrmaker 1993; Yang and Chahande 1995), which assumes an explicit relationship between the density and the material property. In this work, a microstructure-based design domain method proposed by Gea (1996) is applied to model the stiffener location problem and the resulting optimum problem is solved by a sequential convex approximation method called generalized convex approximation (Chickermane and Gea 1996). The solution procedure of stiffener location problem is shown in the flowchart in Fig. 1. A finite element method package, MSC/NASTRAN, is incorporated into the analysis module. In the following sections, we will briefly discuss every module in the first phase.

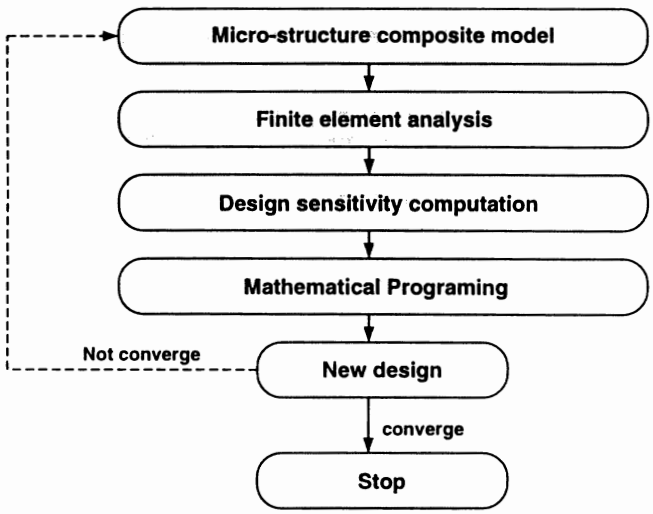

Fig. 1. Phase 1: solution procedure of stiffener location problem

2.1 *Microstructure-based modelling*

In the microstructure-based design domain method, the design domain is discretized into elements which are made of a composite material consisting of spherical micro-inclusions embedded in a solid matrix. The volume fractions of inclusion material in each of design cells are considered as the design variables. For the stiffener location problem, one can simply treat the base material as the matrix phase and stiffener material as the inclusion phase. The optimal stiffener location can be identified by the final distribution of inclusion materials.

The choice of spherical inclusions in an isotropic matrix ensures that the shape and orientation of the inclusion do not enter the problem formulation. The derivation of the relation between the material properties and volume fractions is based on the work by Weng (1984), who obtained the effective material properties using the Mori-Tanaka mean field theory (1973) in conjunction with Eshelby's (1957) equivalence principle and the solution for an ellipsoidal inclusion. For a composite material with a volume fraction x_i of the spherical inclusion, the effective material properties of the composite are

$$\frac{\kappa_i}{\kappa_0} = 1 + \frac{x_i(\kappa_1 - \kappa_0)}{(1 - x_i)\alpha_0(\kappa_1 - \kappa_0) + \kappa_0}, \tag{1}$$

$$\frac{\mu_i}{\mu_0} = 1 + \frac{x_i(\mu_1 - \mu_0)}{(1 - x_i)\beta_0(\mu_1 - \mu_0) + \mu_0}, \tag{2}$$

where κ and μ are bulk and shear modulus, indices i represent the i-th design element, 0 and 1 refer to the matrix and inclusion material respectively, and

$$\alpha_0 = \frac{1}{3}\frac{1 + \nu_0}{1 - \nu_0}, \tag{3}$$

$$\beta_0 = \frac{2}{15}\frac{4 - 5\nu_0}{1 - \nu_0}. \tag{4}$$

Assuming the ratio of Young's modulus of the inclusion and matrix as $E_1/E_0 = r$, we obtain the effective Young's modulus as

$$E_i = -\frac{8(r-1)^2 x_i^2 + (23r^2 - 7r - 16)x_i + (14r^2 + 23r + 8)}{8(r-1)^2 x_i^2 + 6(r^2 - r)x_i + (-14r^2 - 23r - 8)} E_0 \tag{5}$$

The advantages of this method are that it is derived from the rigorous formulation of the theory of composite materials and gives a closed-form expression for the effective Young's modulus which is relatively simple to use.

2.2 *Optimum problem formulation*

The microstructure-based model is utilized to formulate the optimization problem that can be solved by mathematical programming. The structure is first discretized into a number of design elements. For static problems, the most common design objective is to minimize the mean compliance of the structure with a constraint on the volume of the stiffener material to be used. The mean compliance is defined as

$$\Pi = \int_{\Omega} f u \, \mathrm{d}\Omega + \int_{\Gamma_t} t u \, \mathrm{d}\Gamma, \tag{6}$$

where f represents the body forces applied to the structure Ω, t is the traction forces acting on the boundary Γ_t and u is the solution for the displacement of the structure obtained from the equilibrium equations. Minimizing the mean compliance will lead to a design of maximum stiffness under fixed loading. For dynamic applications the design objective is often to maximize the eigenvalue of a specified mode in order to avoid the structural resonances.

Therefore, the optimization problem for stiffener location can be formulated as

$$\text{minimize} \quad \Pi \quad \text{or} \quad -\lambda_n, \tag{7}$$

$$\text{subject to} \quad \int_{\Omega} x_i \, \mathrm{d}\Omega \le \Omega_s, \tag{8}$$

where Π is the objective function for static problems and λ_n, the n-th structural eigenvalue, is for dynamic problems and Ω_s stands for the upper bound of the given stiffener material.

2.3 *Design sensitivity computation*

Once the design problem is formulated, we need to determine the effect resulting from a small perturbation in the current design on the objective and constraint functions, which is known as sensitivity analysis. Using the finite element formulation, the sensitivity of mean compliance can be expressed as

$$\frac{\partial \Pi}{\partial x_i} = -\mathbf{u}^T \frac{\partial \mathbf{K}}{\partial x_i}\mathbf{u} = -u_i^T \frac{\partial [\mathbf{K}_i]}{\partial x_i} u_i, \tag{9}$$

where $\mathbf{K}$ is the global stiffness matrix for the structure; u_i represents the displacement components in the i-th element

and $[\mathbf{K}_i]$ is the i-th element stiffness matrix. The eigenproblem of a structure system can be written as

$$\mathbf{K}\psi_j = \lambda_j \mathbf{M}\psi_j\,, \tag{10}$$

where λ_j is the j-th eigenvalue, which is assumed to be a nonrepeated one, ψ_j is the corresponding eigenvector. Taking the first derivative of (10) with respect to the design variable x_i

$$\frac{\partial \lambda_j}{\partial x_i}\mathbf{M}\psi_j = (\mathbf{K} - \lambda_j \mathbf{M})\frac{\partial \psi_j}{\partial x_i} + \left(\frac{\partial \mathbf{K}}{\partial x_i} - \lambda_j \frac{\partial \mathbf{M}}{\partial x_i}\right)\psi_j\,. \tag{11}$$

Multiplying both sides of (11) by ψ_j^T, and making use of (10) and the mass normalization condition $\psi_j{}^T \mathbf{M}\,\psi_j = 1$, we obtain

$$\frac{\partial \lambda_j}{\partial x_i} = \psi_j^T \left(\frac{\partial \mathbf{K}}{\partial x_i} - \lambda_j \frac{\partial \mathbf{M}}{\partial x_i}\right)\psi_j =$$

$$\psi_{j,i}^T \left(\frac{\partial [\mathbf{K}_i]}{\partial x_i} - \lambda_j \frac{\partial [\mathbf{M}_i]}{\partial x_i}\right)\psi_{j,i}\,, \tag{12}$$

where $\psi_{j,i}$ represents the component of the j-th eigenvector with respect to the i-th element; $[\mathbf{K}_i]$ and $[\mathbf{M}_i]$ are the i-th element stiffness matrix and mass matrix, respectively.

Using the relation derived from the microstructure-based model, $\partial[\mathbf{K}_i]/\partial x_i$ is ready to be evaluated; the element mass matrix is assumed to be a linear function of the add-on stiffener material as $[\mathbf{M}_i] = (1 + x_i)[\mathbf{M}_{i0}]$ where $[\mathbf{M}_{i0}]$ is the i-th element mass matrix of base structure. In this way, the term $\partial[\mathbf{M}_i]/\partial x_i$ is also easy to obtain. After the design sensitivity information for the objective function and constraints are calculated, the generalized convex approximation (GCA) method introduced by Chickermane and Gea (1996) is used to formulate an approximated optimization problem and it is then solved iteratively using mathematical programming until the optimized stiffener location is generated.

3 Phase II: optimal stiffener orientation

Once the location of the stiffener is determined, we need to find the optimal orientation of stiffeners. As we can find from Fig. 2, a stiffened shell has very complicated geometry that is associated with the stiffener orientation. Although it is possible to model it as ensembles of several smaller elements, remeshing of the model would be inevitable during the process of searching its optimal orientation.

To overcome this difficulty, we derived a bending equivalent orthotropic model instead of dealing directly with the original stiffened shell because the orthotropic model only involves the change of the material properties when the stiffener rotates. In this section, a bending equivalent orthotropic model is first derived and then the optimality criteria for the optimal stiffener orientation are established and solved using an energy-based method.

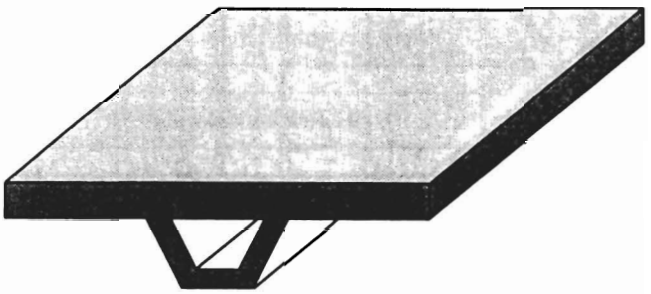

Fig. 2. Stiffened shell design cell

3.1 Bending equivalent orthotropic model

In a shell/plate structure problem, the constitutive equations are required to relate the stress resultants and stress couples, instead of merely stresses, to the corresponding strains and curvatures. If we neglect the membrane-bending coupling effect, for a base shell element with Young's modulus E, Possion's ratio ν, and uniform thickness t, the stress resultant-strain and stress couple-curvature relations can be represented as

$$\begin{Bmatrix} \mathbf{N}_m \\ \mathbf{M}_b \\ \mathbf{Q}_s \end{Bmatrix} = \begin{bmatrix} \mathbf{D}_m & 0 & 0 \\ 0 & \mathbf{D}_b & 0 \\ 0 & 0 & \mathbf{D}_s \end{bmatrix} \begin{Bmatrix} \varepsilon_m \\ \kappa_b \\ \gamma_s \end{Bmatrix}, \tag{13}$$

where $\mathbf{N}_m$ is the in-plane membrane force vector, $\mathbf{M}_b$ is the flexural moment vector, and $\mathbf{Q}_s$ is the transverse shear force vector; ε_m stands for the in-plane strains, κ_b represents the curvatures, and γ_s stands for the transverse shear strains; $\mathbf{D}_m$ represents the membrane stiffness, $\mathbf{D}_b$ is the flexural rigidity, and $\mathbf{D}_s$ is the transverse shear stiffness.

The flexural rigidity $\mathbf{D}_b$ of the base shell can be expressed in an explicit form as

$$\mathbf{D}_b = \begin{bmatrix} \dfrac{Et^3}{12(1-\nu^2)} & \dfrac{\nu Et^3}{12(1-\nu^2)} & 0 \\ \dfrac{\nu Et^3}{12(1-\nu^2)} & \dfrac{Et^3}{12(1-\nu^2)} & 0 \\ 0 & 0 & \dfrac{Et^3}{24(1+\nu)} \end{bmatrix}. \tag{14}$$

To formulate the stress resultant-strain and stress couple-curvature relations of a stiffened shell, it is economical to derive its equivalent thicknesses. One promising approach for this equivalence problem is the split rigidity concept introduced by Buchert (1973). In the split rigidity concept, different equivalent thicknesses for the extensional, shearing, bending, and twisting terms are specified. For the stiffened shell, the equivalent extensional thicknesses, shear thickness and twisting thickness are very close to the base structure thickness t because the stiffener has little effect on them. However, due to the alteration of the shell section geometry caused by the addition of the stiffener, the bending rigidity in the direction where the stiffener runs is increased drastically. The equivalent bending thickness can be approximated as $t_b = (12 I_b/\ell)^{1/3}$ where I_b and ℓ are the moment of inertia and the length of the stiffened shell section. Since I_b is much

larger than the moment of inertia of the base shell section, t_b is normally several times that of the base thickness. In this research, we will not look into the detailed configurations of stiffeners; the stiffener geometry in each design cell is assumed to be known beforehand in the form of its equivalent bending thickness t_b.

The flexural rigidity $\mathbf{D}_b$ of the stiffened shell can be obtained by superseding the base thickness t with t_b in the bending term as

$$\mathbf{D}_b = \begin{bmatrix} \frac{Et_b^3}{12(1-\nu^2)} & \frac{\nu Et^3}{12(1-\nu^2)} & 0 \\ \frac{\nu Et^3}{12(1-\nu^2)} & \frac{Et^3}{12(1-\nu^2)} & 0 \\ 0 & 0 & \frac{Et^3}{24(1+\nu)} \end{bmatrix}, \tag{15}$$

where E is Young's modulus and ν is Poisson's ratio.

In order to find a bending equivalent orthotropic model for the stiffened shell element, we consider the flexural rigidity of an orthotropic shell with elastic constants c_{ij}^0 and uniform thickness t. The flexural rigidity $\mathbf{D}_b$ of the orthotropic shell element can be written as

$$\mathbf{D}_b = \begin{bmatrix} \frac{c_{11}^0 t^3}{12} & \frac{c_{12}^0 t^3}{12} & 0 \\ \frac{c_{12}^0 t^3}{12} & \frac{c_{22}^0 t^3}{12} & 0 \\ 0 & 0 & \frac{c_{33}^0 t^3}{12} \end{bmatrix}. \tag{16}$$

Since two shell elements are bending equivalent if they have the same flexural rigidity, a bending equivalent orthotropic model of the stiffened shell element can be constructed by making the flexural rigidity in the above equation equal to that of the stiffened element defined in (15). Equivalent orthotropic material coefficients are determined as follows:

$$c_{11}^0 = \frac{t_b^3}{t^3}\frac{E}{1-\nu^2}, \quad c_{12}^0 = \frac{\nu E}{1-\nu^2},$$

$$c_{22}^0 = \frac{E}{1-\nu^2}, \quad c_{33}^0 = \frac{E}{2(1+\nu)}. \tag{17}$$

Because the membrane stiffness and the transverse shear stiffness of the stiffened shell are the same as those of base element, the base isotropic material is used directly for calculating the extensional and shear deformations. For the flexural deformation computation, the bending equivalent orthotropic model is applied to model each stiffened shell element. In this way, the optimal stiffener orientation problem is transformed rigorously into an optimal orientation problem of orthotropic materials that is relatively simple to solve. In the next section, optimal orientation of orthotropic materials will be derived for both static and dynamic problems, the results will then be extended to our bending equivalent orthotropic model.

3.2 Optimality criteria formulation

For a linear static problem, the mean compliance Π can be expressed as

$$\Pi = \int_\Omega \sigma_{ij}\varepsilon_{ij}\,\mathrm{d}\Omega =$$

$$\int_\Omega C_{ijk\ell}\varepsilon_{ij}\varepsilon_{k\ell}\,\mathrm{d}\Omega = \int_\Omega C_{ijk\ell}\frac{\partial u_i}{\partial x_j}\frac{\partial u_k}{\partial x_\ell}\,\mathrm{d}\Omega, \tag{18}$$

where $C_{ijk\ell}$ is the elastic coefficient of orthotropic material which depends on both material property and orientation variable θ; σ_{ij} and ε_{ij} represent stress and strain components of the structure. The optimality condition of the optimal orientation θ is derived by setting the derivative of the objective function Π with respect to the orientation variable θ to be zero. This leads to

$$\frac{\partial \Pi}{\partial \theta} = \int_\Omega \left[\frac{\partial C_{ijk\ell}}{\partial \theta}\frac{\partial u_i}{\partial x_j}\frac{\partial u_k}{\partial x_\ell} + 2C_{ijk\ell}\frac{\partial}{\partial \theta}\left(\frac{\partial u_i}{\partial x_j}\right)\frac{\partial u_k}{\partial x_\ell}\right]\mathrm{d}\Omega = 0. \tag{19}$$

By taking the first derivative of the weak form of a linear elastostatic problem with respect to the orientation variable θ, we have the following relation:

$$\int_\Omega \frac{\partial C_{ijk\ell}}{\partial \theta}\frac{\partial u_i}{\partial x_j}\frac{\partial u_k}{\partial x_\ell}\,\mathrm{d}\Omega = -\int_\Omega C_{ijk\ell}\frac{\partial}{\partial \theta}\left(\frac{\partial u_i}{\partial x_j}\right)\frac{\partial u_k}{\partial x_\ell}\,\mathrm{d}\Omega. \tag{20}$$

Combining the results of (19) and (20), the optimality condition of a linear elastostatic problem is expressed as

$$\frac{\partial \Pi}{\partial \theta} = -\int_\Omega \frac{\partial C_{ijk\ell}}{\partial \theta}\frac{\partial u_i}{\partial x_j}\frac{\partial u_k}{\partial x_\ell}\,\mathrm{d}\Omega = 0. \tag{21}$$

For a nonrepeated eigenvalue optimization problem, the weak formulation can be written as

$$\int_\Omega C_{ijk\ell}\frac{\partial \phi_i^n}{\partial x_j}\frac{\partial \psi_k}{\partial x_\ell}\,\mathrm{d}\Omega - \lambda_n\int_\Omega \rho\phi_k^n\psi_k\,\mathrm{d}\Omega = 0, \tag{22}$$

where λ_n stands for the n-th eigenvalue of the structure, and ϕ^n represents the corresponding eigenvector; ρ is the material density, and ψ is a virtual system eigenvector in kinematically admissible set. Performing the first partial derivative of (22) with respect to θ gives

$$\int_\Omega \left[\frac{\partial C_{ijk\ell}}{\partial \theta}\frac{\partial \phi_i^n}{\partial x_j}\frac{\partial \psi_k}{\partial x_\ell} + C_{ijk\ell}\frac{\partial}{\partial\,\theta}\left(\frac{\partial \phi_i^n}{\partial x_j}\right)\frac{\partial \psi_k}{\partial x_\ell} - \frac{\partial \lambda_n}{\partial \theta}\rho\phi_k^n\psi_k - \lambda_n\rho\frac{\partial \phi_k^n}{\partial \theta}\psi_k\right]\mathrm{d}\Omega = 0. \tag{23}$$

By setting $\psi_k = \phi_k^n$ and using the mass normalization condition $\int_\Omega \rho\phi_i^n\phi_i^n \, d\Omega = 1$, we can rewrite (23) as

$$\frac{\partial\lambda_n}{\partial\theta} = \int_\Omega \left[\frac{\partial C_{ijk\ell}}{\partial\theta}\frac{\partial\phi_i^n}{\partial x_j}\frac{\partial\phi_k^n}{\partial x_\ell} + C_{ijk\ell}\frac{\partial}{\partial\theta}\left(\frac{\partial\phi_i^n}{\partial x_j}\right)\frac{\partial\phi_k^n}{\partial x_\ell} - \lambda_n\rho\frac{\partial\phi_k^n}{\partial\theta}\phi_k^n \right] d\Omega . \quad (24)$$

Comparing the resulting equation from letting ψ_k be $\partial\phi_k^n/\partial\theta$ in (22), the optimality condition for maximizing λ_n in a dynamic problem is represented as

$$\frac{\partial\lambda_n}{\partial\theta} = \int_\Omega \frac{\partial C_{ijk\ell}}{\partial\theta}\frac{\partial\phi_i^n}{\partial x_j}\frac{\partial\phi_k^n}{\partial x_\ell} \, d\Omega = 0 . \quad (25)$$

Therefore, if we define a function Ψ as Π in the static problems and $-\lambda_n$ in the dynamic problems, a unified optimality condition for both cases is obtained as

$$\frac{\partial\Psi}{\partial\theta} = -\int_\Omega \frac{\partial C_{ijk\ell}}{\partial\theta}\varepsilon_{ij}\varepsilon_{k\ell} \, d\Omega = 0 . \quad (26)$$

If we neglect the membrane-bending coupling effect in (26) for simplicity, the optimality condition can be written as

$$\frac{\partial\Psi}{\partial\theta} = -\int_\Omega \left(\frac{\partial C_{ijk\ell}^m}{\partial\theta}\varepsilon_{ij}^m\varepsilon_{k\ell}^m + \frac{\partial C_{ijk\ell}^b}{\partial\theta}\varepsilon_{ij}^b\varepsilon_{k\ell}^b + \frac{\partial C_{ijk\ell}^s}{\partial\theta}\varepsilon_{ij}^s\varepsilon_{k\ell}^s \right) d\Omega = 0 , \quad (27)$$

where $C_{ijk\ell}^m, C_{ijk\ell}^b, C_{ijk\ell}^s$ are material properties used for membrane, bending and transverse shearing calculations, and $\varepsilon_{ij}^m, \varepsilon_{ij}^b, \varepsilon_{ij}^s$ are the resulting strains, respectively.

For stiffened shell structures simulated by a bending equivalent orthotropic model, the base isotropic material is applied to evaluate the extensional and shearing deformations, and the bending equivalent orthotropic material is employed to calculate the bending curvatures, the first and the third terms of (27) will be zero. If there are m stiffened shell elements in the structure after the first phase and the finite element mesh is fine enough, the bending strain in each design cell can be assumed independent of plane coordinates and it is only a linear function of the distance from the associated point to the mid-surface where the shell remains unbended. Therefore (27) can be modified as

$$\frac{\partial\Psi}{\partial\theta_e} = -\frac{1}{3}\boldsymbol{\varepsilon}_e^T\frac{\partial\mathbf{C}}{\partial\theta_e}\boldsymbol{\varepsilon}_e A^e t = 0 , \quad e = 1, 2, \ldots, m , \quad (28)$$

where $\boldsymbol{\varepsilon}_e$ represents the strain vector of the e-th design cell on the upper face, and it is an implicit function of orientation variables in all design cells; A^e stands for the area of the e-th design cell, and t is the base thickness. For simplicity, $\frac{1}{3}A^e t$ will be set to be unity thereafter; $\mathbf{C}$ is the equivalent rotated orthotropic stiffness matrix of the e-th design cell and it is defined as, $\mathbf{C} = \mathbf{T}^T(\theta_e)\mathbf{C}_0\mathbf{T}(\theta_e)$, where $\mathbf{C}_0$ stands for the unrotated orthotropic stiffness matrix, and $\mathbf{T}(\theta_e)$ is a standard rotation matrix.

3.3 Energy-based method

It should be noted that (28) is one set of coupled equations since strain $\boldsymbol{\varepsilon}_e$ is an implicit function of the orientation variables for all design cells. To solve these equations, further simplifications must be made. To this end, a newly developed method, the energy-based method, will be briefly discussed in this section. For the details of the energy-based method, please refer to the paper by Luo and Gea (1997). In the energy-based method, the strain field of one design cell is assumed as a function of its own orientation. The coupling effect, i.e. the dependency of strain field on the material orientation of the surrounding cells, is assumed to be insignificant and therefore neglected. By applying an inclusion model, the strain $\boldsymbol{\varepsilon}_e$ of the e-th design cell after rotation can be evaluated as

$$\boldsymbol{\varepsilon}_e = (1-\alpha)\boldsymbol{\varepsilon}_0 + \alpha\mathbf{S}\boldsymbol{\sigma}_0 , \quad (29)$$

where $\boldsymbol{\varepsilon}_0$ and $\boldsymbol{\sigma}_0$ are the initial strain and stress fields of the e-th design cell, $\mathbf{S}$ is the rotated orthotropic compliance matrix and α is the energy factor which is defined as the ratio of strain energy stored in the design cell to that of the whole structure due to the work done by a traction force at the interface.

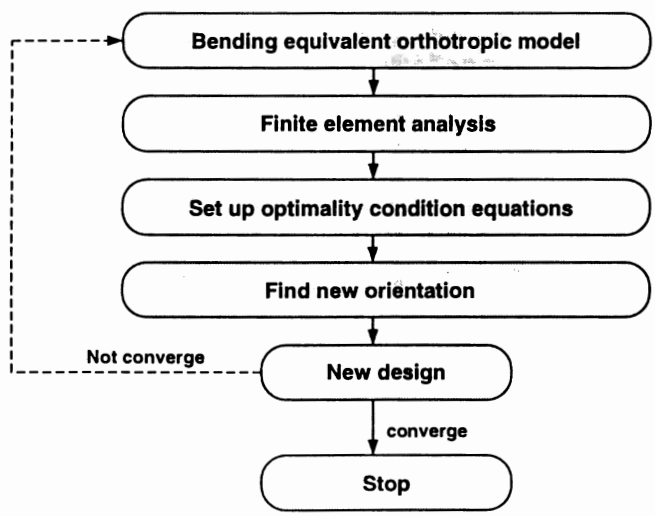

Fig. 3. Phase 2: solution procedure of stiffener orientation problem

Introducing the above expression into the optimality conditions of (28), a set of uncoupled equations in terms of orientation variables $\theta_e, e = 1, 2, \ldots, m$ can be obtained as

$$\frac{\partial\Psi}{\partial\theta_e} = (-1+2\alpha-\alpha^2)\boldsymbol{\varepsilon}_0^T\frac{\partial\mathbf{C}}{\partial\theta_e}\boldsymbol{\varepsilon}_0 + \alpha^2\boldsymbol{\sigma}_0^T\frac{\partial\mathbf{S}}{\partial\theta_e}\boldsymbol{\sigma}_0 + (2\alpha^2-2\alpha)\boldsymbol{\varepsilon}_0^T\frac{\partial\mathbf{C}}{\partial\theta_e}\mathbf{S}\boldsymbol{\sigma}_0 = 0 . \quad (30)$$

Two previously developed methods, the strain-based method (Pedersen 1989, 1990, 1991; Cheng and Pedersen 1997) and the stress-based method (Suzuki and Kikuchi 1991; Diaz and Bendsøe 1992; Cheng *et al.* 1994) can be recovered

from the above equations if we choose $\alpha = 0$ and $\alpha = 1$, respectively. From the physical meaning of the energy factor, $\alpha = 0$ means that the traction force does not do any work on the design cell, this can only be true when the surrounding body is extremely stiff compared to the design cell; $\alpha = 1$ means the traction force does not do any work to the surroundings, which can be only possible when the design cell is much stiffer than its surrounding structure. Normally, the material properties of the design cell and surroundings are comparable, therefore α is a value between 0 and 1. In the current implementation, the energy factor is dynamically determined as $\alpha = ||\sigma_e - C\epsilon_0||/||\sigma_0 - C\epsilon_0||$ at each iteration with an initial estimate value of 0.75.

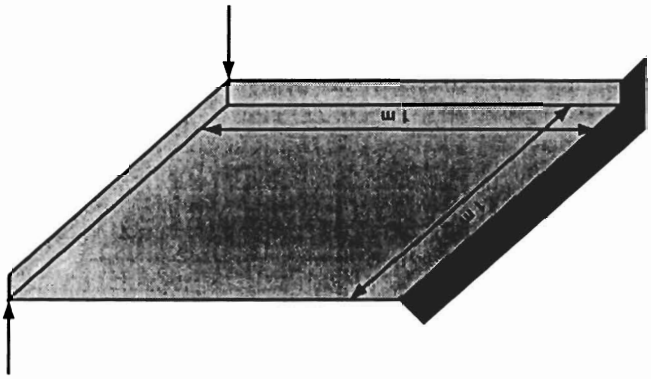

Fig. 4. A plate clamped at one side subjected to a pair of transverse forces

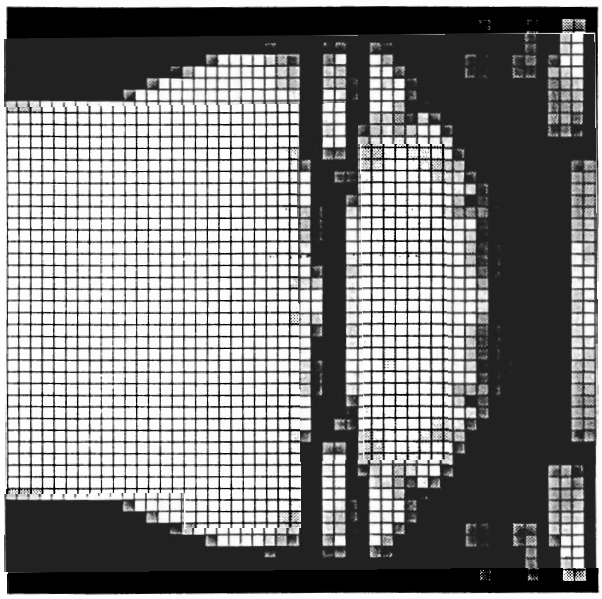

Fig. 5. Stiffener location in square plate

Of the several roots of (30), the desired orientation angle is the one in the interval $(-\frac{\pi}{2}, \frac{\pi}{2})$ that minimizes Ψ, which can be evaluated by the integral of the right-hand side of (30). It should be noted that (30) must be solved iteratively

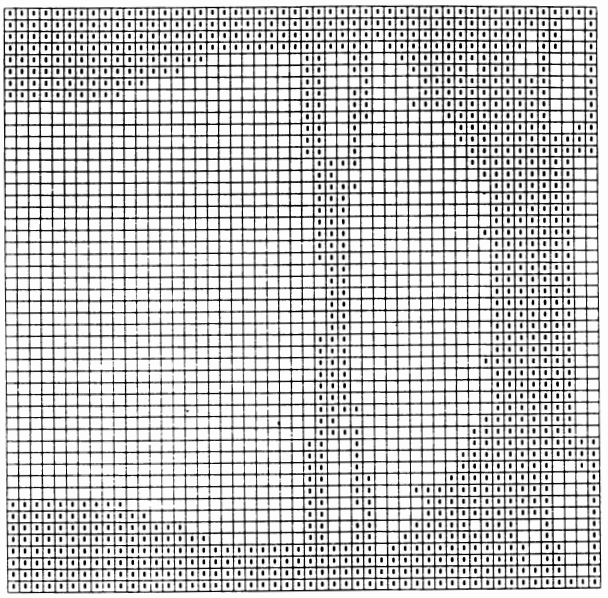

Fig. 6. Stiffener design domain of a square plate

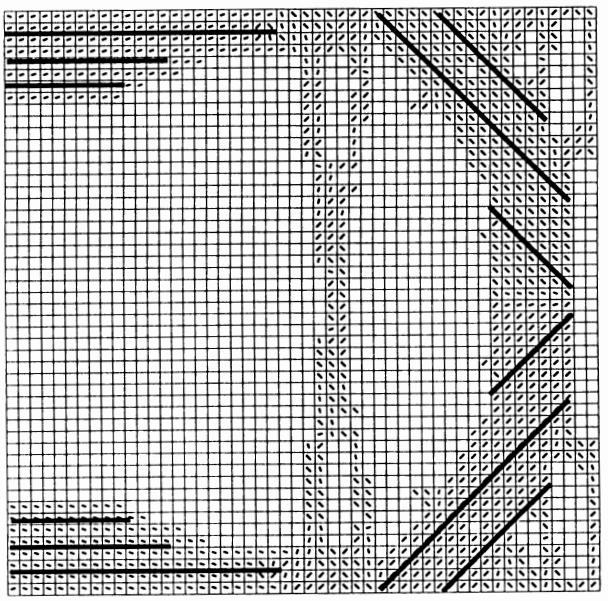

Fig. 7. Stiffener pattern of a square plate

in order to achieve the optimal orientation, but generally convergence can be obtained within a small number of iterations. The solution procedure of the stiffener orientation problem is shown in the flowchart in Fig. 3.

4 Numerical examples

In this section, two numerical examples are presented. The first example is to find the stiffest stiffener configurations of a square plate; the second example is to find the optimal stiffener design for a ruled-surface shell with a design objective of maximizing the eigenvalue of its first mode.

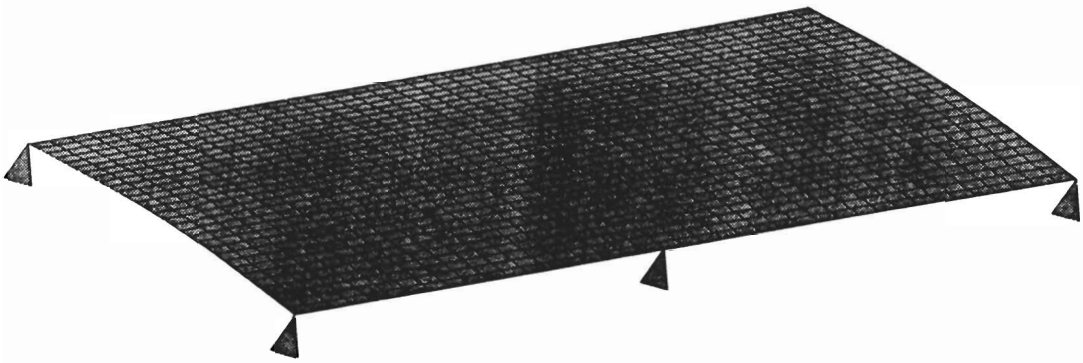

Fig. 8. A curved shell fixed at six points

4.1 Example 1

A square plate of 1 m × 1 m is clamped at one side, and is subjected to a pair of concentrated loads acting along opposite directions at the corners of free ends as shown in Fig. 4. The thickness of the plate is 0.5 cm. Young's modulus of the base material is $E_0 = 80$ GPa, and Poisson's ratio $\nu = 0.3$. The design objective is to minimize the mean compliance of the structure, consequently to maximize the stiffness of the structure.

The stiffener location problem is first solved. Suppose the available volume of stiffener material is 2/5 of the total volume, and the ratio of the stiffener Young's modulus to that of the base Young's modulus r is 1000. The optimal material distribution is shown in Fig. 5 from the first phase. It is found that the stiffener materials are mainly concentrated in the regions which directly connect the loading points and from the loading points to the nearest fixed points. A "cross beam" like stiffener appears in the final layout, which makes the whole plate more stable under the torsional load.

From the result of the stiffener location optimization in Fig. 5, a total number of 1000 stiffened design cells are identified in Fig. 6. Suppose the equivalent bending thickness of each design cell is twice that of the base structure after particular stiffeners are constructed. Figure 7 shows the optimal stiffener design of the square plate after the second phase. As we can see in the figure, the stiffeners near the fixed points appear to be horizontal, and the stiffeners in the rightmost region are oriented at approximately 45 degrees to the horizontal level. With this stiffener design, the mean compliance is reduced to only half of that corresponding to the initial design where all stiffeners are held vertically (Fig. 6). Comparing with the original structure without stiffener, the stiffness of the final structure increases nearly 50 times with the mean compliance value decreased from 8.9273×10^{-2} Nm to 4.7476×10^{-4} Nm.

4.2 Example 2

A ruled-surface shell has a base 2 m by 1.5 m. The longer sides of the shell are straight lines and the shorter sides are lifted up 2 cm in the centre and form two parabolic lines. The shell is fixed at six points as shown in Fig. 8. Young's modulus of the base material is $E_0 = 200$ GPa, the density $\rho_0 = 7850$ kg/m^3, and Poisson's ratio $\nu = 0.3$. The objective is to find the optimal stiffener design in order to maximize the first eigenvalue.

The stiffener location problem is first carried out in the first phase. Suppose that the available volume of stiffener material is 1/2 of the total volume, and the ratio of stiffener Young's modulus to that of base Young's modulus r is 1000. The optimal stiffener distribution is shown in Fig. 9. It is found that the stiffener materials are mainly concentrated in the vicinity of fixed points and two straight stiffeners are clearly identified.

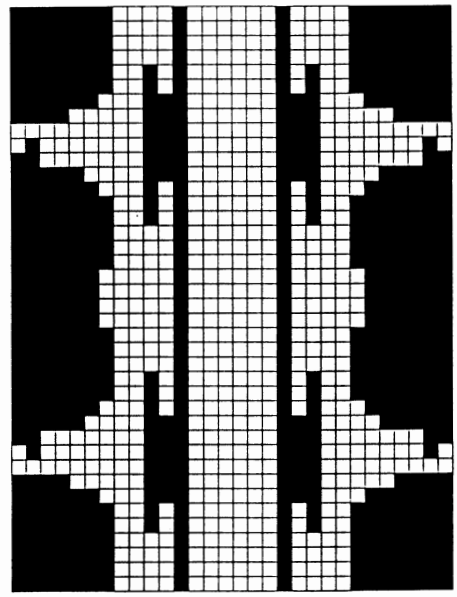

Fig. 9. Stiffener location in a curved shell structure

There are a total of 600 stiffened design cells in this problem as shown in Fig. 10. The equivalent bending thickness of each design cell is assumed to be twice that of the base structure after particular stiffeners are placed. The optimal stiffener design result is shown in Fig. 11, where arc-type stiffeners can be easily identified around the four corner points; the radiant-type stiffeners and then arc-type stiffeners are located in the vicinities of the two centre points, and two vertical stiffener lines are in the middle. With this optimal

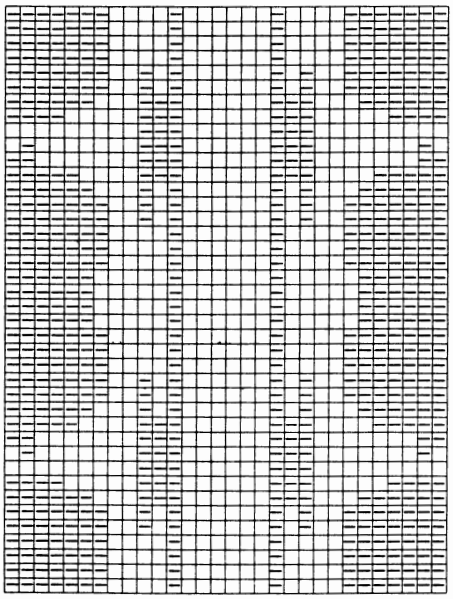

Fig. 10. Stiffener design domain in a curved shell structure

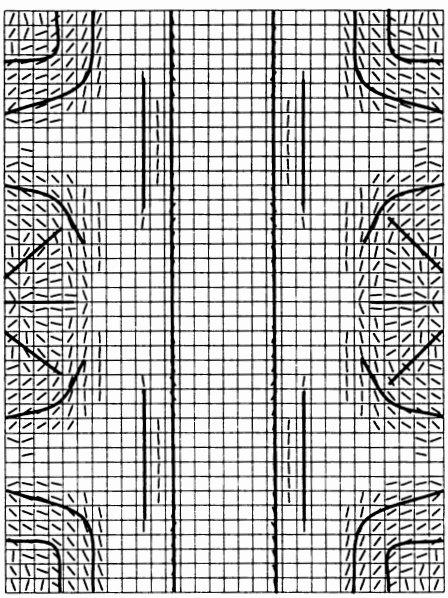

Fig. 11. Stiffener pattern in a curved shell structure

stiffener pattern, the first structural eigenvalue is 131.39 corresponding to 59.79 of the initial structure with all the stiffeners placed horizontally. The first eigenvalue of the structure without stiffeners is 23.71. This shows that a great improvement of the first structural eigenvalue can be achieved by the proper placement of stiffeners.

It should be noted that the eigenfrequencies might switch order in the optimization process of the eigenvalue problem. In that case, a mean eigenvalue, which is a combination of switched eigenvalues, can be used as the objective function; the solution procedure based on the mean eigenvalue can be derived in the same manner as for a single eigenvalue. Since no eigenfrequency switch-over takes place in our examples, we will not elaborate on the mean eigenvalue solution in this paper.

5 Conclusion and discussion

In this paper, a systematic topology optimization approach is developed to assist the optimal stiffener design of a 3D shell/plate structure. The optimal stiffener location is first identified and the stiffener orientation problem is then explored. The stiffened shell is transformed into a bending equivalent orthotropic model and the optimal orientation is obtained by an energy-based method. Case studies of both static and dynamic problems showed that a significant improvement of structural behaviour can be achieved by properly located and oriented stiffeners.

In this paper, we treat the stiffener location problem and orientation problem separately instead of solving them simultaneously. This treatment eliminates the numerical complexity otherwise involved and provides a very simple and straightforward design approach. However, the proposed approach may introduce inaccuracy in dealing with design problems where stiffener location is strongly coupled with orientation. A more sophisticated composite model is currently under development in order to incorporate both stiffener density and orientation.

References

Bendsøe, M.P.; Kikuchi, N. 1988: Generating optimal topologies in structural design using a homogenization method. *Comp. Meth. Appl. Mech. Engrg.* **71**, 197-224

Bendsøe, M.P. 1989: Optimal shape design as a material distribution problem. *Struct. Optim.* **1**, 193-202.

Buchert, K.P. 1973, *Buckling of shell and shell-like structures.* Columbia Academic Publishers

Cheng, G.; Pedersen, P. 1997: On sufficiency conditions for optimal design based on extremum principles of mechanics. *J. Mech. Phys. Solids* **45**, 135-150

Cheng, H.C.; Kikuchi, N.; Ma, Z.D. 1994: An improved approach for determining the optimal orientation of orthotropic material. *Struct. Optim.* **8**, 101-112

Chickermane, H.; Gea, H.C. 1996: A new local function approximation method for structural optimization problems. *Int. J. Numer. Meth. Engrg.* **39**, 829–846

Diaz, A.R.; Bendsøe, M.P. 1992: Shape optimization of structures for multiple loading conditions using a homogenization method. *Struct. Optim.* **4**, 17-22

Diaz, A.R.; Kikuchi, N. 1992: Solutions to shape and topology eigenvalue optimization problems using a homogenization method. *Int. J. Numer. Meth. Engrg.* **35**, 1487-1502

Eshelby, J. 1957: The determination of the elastic field of an ellipsoidal inclusion and related problems. *Proc. Roy. Soc.* **A241**, 379-396

Gea, H.C. 1996: Topology optimization: A new micro-structure based design domain method. *Comp. & Struct.* **61**, 781-788

Luo, J.H.; Gea, H.C.: Optimal orientation of orthotropic materials using an energy based method. *Struct. Optim.* (in press)

Ma, Z.D.; Kikuchi, N.; Hagiwara, I. 1993: Structural topology and shape optimization for a frequency response problem. *Comp. Mech.* **13**, 157-174

Mlejnek, H.P.; Schirrmaker, R. 1993: An engineer's approach to optimal material distribution and shape finding. *Comp. Meth. Appl. Mech. & Engrg.* **106**, 1-26

Mori, T.; Tanaka, K. 1973: Average stress in matrix and average elastic energy of materials with midfitting inclusions. *ACTA Metallurgica* **21**, 571-574

Pedersen, P. 1989: On optimal orientation of orthotropic materials. *Struct. Optim.* **1**, 101-106

Pedersen, P. 1990: Bounds on elastic energy in solids of orthotropic materials. *Struct. Optim.* **2**, 55-63

Pedersen, P. 1991: On thickness and orientational design with orthotropic materials. *Struct. Optim.* **3**, 69-78

Rozvany, G.I.N.; Zhou, M. 1990: Application of the COC method in layout optimization. In: Eschenauer, H.; Matteck, C.; Olhoff, N. (eds.) *Proc. Int. Conf. on Engineering Optimization in Design Processes*, pp. 59-70

Suzuki, K.; Kikuchi, N. 1991: A homogenization method for shape and topology optimization. *Comp. Meth. Appl. Mech. & Engrng.* **93**, 291-318

Weng, G.J. 1984: Some elastic properties of reinforced solids, with special reference to isotropic ones containing isotropic inclusions. *Int. J. Engrg. Sci.* **22**, 845-856

Yang, R.J.; Chahande, A.I. 1995: Automotive application of topology optimization. *Struct. Optim.* **9**, 245-249

Received March 9, 1998
Revised version received June 10, 1998

Announcement

International Centre for Mechanical Sciences (CISM)
Preliminary Programme 1999

Damage Mechanics: Statistical Aspects
Coordinators: D. Krajcinovic (Arizona)
J. van Mier (Delft) May 31-June 4

Rolling Contact Phenomena
Coordinator: J.J. Kalker (Delft) June 21-25

IUTAM-CISM-HYDROMAG Advanced School on
Liquid Metal Magnetohydrodynamics
Coordinators: P. Davidson (Cambridge),
A. Thess (Dresden) June 21-25

Deployable Structures
Coordinator: S. Pellegrino (Cambridge) July 5-9

Fretting Fatigue
Coordinators: J. Dominguez (Sevilla),
T. Lindley (London) July 12-16

Bone Cell and Tissue Mechanics
Coordinator: S.C. Cowin (New York) July 19-23

Material Instabilities in Elastic and Plastic Solids
Coordinator: H. Petryk (Warsaw) September 13-17

Advanced Professional Training
Semirigidity in Connections of Structural Steelworks: Theory, Analysis and Design
Coordinators: M. Ivanyi (Budapest)
C.C. Baniotopoulos (Thessaloniki) September 20-24

Turbulence Modulation and Control
Coordinator: A. Soldati (Udine) September 20-24

Adaptive Finite Elements in Linear and
Nonlinear Solid and Structural Mechanics
Coordinator: E. Stein (Hannover) October 4-8

Environmental Geomechanics
Coordinator: B. Schrefler (Padua) October 11-15

Advanced Professional Training
Seismic Resistant Steel Structures:
Progess and Challenge
Coordinators: F.M. Mazzolani (Naples),
V. Gioncu (Timisoara) October 18-22

Palazzo del Torso, Piazza Garibaldi 18, 33100 Udine, Italy
tel.: +39 0432248511 (6 lines) - fax 0432248550 - e-mail: cism@uniud.it - http://www.uniud.it/cism/homepage.htm